Journal of Molecular Graphics and Modelling 72 (2017) 106–111

Contents lists available at ScienceDirect

Journal of Molecular Graphics and Modelling

journal homepage: www.elsevier.com/locate/JMGM

Enhancing 4-propylheptane dissociation with nickel nanocluster based on molecular dynamics simulations

Margarita G. Ilyina[a,c,*], Edward M. Khamitov[a,b,c], Rail N. Galiakhmetov[d], Ildar A. Mustafin[e], Akhat G. Mustafin[a]

[a] Bashkir State University, Chemical Faculty, Department of Physical Chemistry and Chemical Ecology, 32 Zaki Validi Str., Ufa 450074, Russia
[b] Ufa Institute of Chemistry, Russian Academy of Sciences, Laboratory of Chemical Physics, 69 Prospekt Oktyabrya, Ufa 450054, Russia
[c] Institute of Petroleum Refining and Petrochemistry, Laboratory of quantum chemistry and molecular dynamics of the Department of Chemistry and Technology, 12 Initsiativnaya Str., Ufa 450065, Republic of Bashkortostan, Russia
[d] Bashkir State University, Engineering College, Department of Quality Management, 100 Mingageva Str., Ufa 450078, Russia
[e] Ufa State Petroleum Technological University, Technological Faculty, Department of Oil and Gas Technology, 1 Kosmonavtov Str., Ufa 450062, Russia

ARTICLE INFO

Article history:
Received 3 October 2016
Received in revised form 2 December 2016
Accepted 29 December 2016
Available online 3 January 2017

Keywords:
Density functional theory
Hybrid exchangecorrelation functionals
Molecular orbitals
Small metallic clusters
Atoms in molecule
HOMO/LUMO-gap
Ab initio molecular dynamics

ABSTRACT

In the present work, a 0.4 nm nickel cluster has been theoretically studied. Its equilibrium structural parameters have been calculated by the DFT method based on the PBEH1PBE hybrid functional and split-valence basis set Lanl2DZ including effective core potentials. We have systematically considered diverse spin states of this cluster and find out its ground state. The relative stability of these states depends on the HOMO–LUMO gap. The interaction of the Ni_6 with 4-propylheptane $C_{10}H_{22}$ has been studied to simulate the process of catalytic cracking of hydrocarbons. The optimization of this structure has been performed by the ωPBE/Lanl2DZ_ecp method (the TeraChem V.1.9 program package) with no symmetry restrictions; the electron shells of the metal were described by effective core pseudopotentials. For visualization and quantitative estimation of the bonding bonds between the nickel nanocluster and 4-propylheptane, the analysis of weak interactions based on RGD has been performed. To confirm the proposition about the formation of Ni–H bonds, we have scrutinized critical points of electronic density. Values of laplasian of electronic density and Bader atomic charge distribution in the global minimum of the total energy have been estimated by the AIMAll 15.05.18 program suite. Finally, we have simulated interaction of Ni_6 with 4-propylheptane in terms of the Born–Oppenheimer *ab initio* molecular dynamics. The results of the molecular dynamics simulation provide pair radial distribution function C—H at 1500 °C and a detailed picture of the processes occurring in the system.

1. Introduction

The catalytic cracking of vacuum gas oil is one of the basic processes in the refinery as it resolves the following problems: an increase in the depth of oil refining, production of semi-finished diesel fuel (one of the most important components of high total gasoline pool at the refinery) and precursors for the petrochemical industry. Catalysts for modern cracking processes, which are carried out at high temperatures under intensive mass and heat transfer in apparatus with a moving or fluidized catalyst bed, must possess the enhanced regenerative, mechanical and other performance characteristics in addition to the high selectivity and thermal stability. Currently, there is a considerable interest in transition metal clusters. This interest comes from the experimental and theoretical perspectives because the transition metal clusters are unique systems, intermediate between molecules and solids. Small metal nanoclusters play an important role in the homogeneous formation of active centers, crystal growth, formation of amorphous materials, atmospheric chemistry processes, and heterogeneous catalysis [1,2]. Recently, nanocatalysts are recognized as a promising alternative, which combines the advantages of both homo- and heterogeneous catalysts with pronounced unique activity. Properties of nanocatalysts drastically depend on their shape, size, chemical composition, and morphology of the active nanoparticles. In recent decades, significant efforts have been focused on designing and manufacturing the tunable nanostructured catalytic materials. As mentioned above, transition metal clusters are

* Corresponding author. Present address: Bashkir State University, Chemical Faculty, Department of Physical Chemistry and Chemical Ecology, 32 Zaki Validi Str Ufa 450074, Russia.
E-mail address: margarita.kondrova@yandex.ru (M.G. Ilyina).

http://dx.doi.org/10.1016/j.jmgm.2016.12.017
1093-3263/

an important class of nanocatalysts with several unique features. Their ability to serve as catalysts is determined by several factors: 1) high ratio of surface area to volume; 2) the presence of the active absorption and reaction sites; 3) low energetic barriers for restructurization; 4) a wide range of coordination numbers; 5) the possibility of light atomic rearrangements greatly facilitating the cleavage of chemical bonds.

The geometry of transition metal clusters is undoubtedly an important factor defining their physical and chemical properties. In recent years, studies of metallic clusters provided significant advances but the main task of determining the geometric structure of the cluster remains unresolved. Unfortunately, the size of the clusters of greatest interest (3–100 atoms) are too large for typical spectrophotometric methods and too small for electron microscopy techniques. As for theoretical studies, computations of the transition metal systems meet a problem for their theoretical description due to the presence of several nearly placed orbital levels in transition metal atoms [3,4]. Therefore, molecules and clusters containing transition metals require an accurate search for appropriate theoretical methods [5]. Among transition metals, nickel clusters has received the most attention, both experimental and theoretical. Nickel atom has a strongly bound d-electron shell, which contribution to the metallic bond may be relatively small [6]. Thus, the calculations neglecting the contribution of d-orbitals in metallic bonds are able to provide an appropriately accurate prediction of the cluster structure. Over the past three decades, small clusters of nickel and their properties have attracted great interest of researchers [7]. Several experimental studies have been devoted to nickel clusters. In addition, a significant number of theoretical studies of small clusters of nickel has been performed [8–10]. The development of modern nanotechnology and an increased industry interest in the creation of new technical devices has induced the need for a detailed study of the characteristics of small metal particles [11]. Numerous studies have shown that reducing the particle size to the nanometer range contributes to the manifestation of entirely new properties (thermodynamic, chemical, mechanical, magnetic, etc.) which are caused not only by a high ratio of surface to volume of the nanoparticles, but with the type of crystal nanocluster configuration [12]. Such effects are most clearly observed when the size of the obtained grains or clusters is less than 10 nm [13,14]. However, the commercialization of the use of nanoparticles encounters serious limitations associated with the apparent lack of theoretical knowledge. Experimental techniques for observing the structure of small metal clusters have existed for a long time but have many disadvantages and, hence, computer simulation remains an indispensable tool for the study of the internal structure of nanoparticles. Therefore, in the present work, we have performed an accurate theoretical study of small nickel clusters using density functional theory [15–20]. To define the ground states, diverse spin states (singlet, triplet, quintet, septet, nonet, undecimet) were tested for each type of the clusters.

2. Computational details

Quantum-chemical modeling of the equilibrium geometric parameters for the cluster Ni_6 was performed by density functional theory (DFT) with the *ab initio* local functional PBE [21,22] (Perdew–Burke– Ernzerhof) with the Lanl2DZ [23–26] split-valence basis set comprising effective core potentials. The chosen computational method, as demonstrated by previous tests, accurately reproduces the structure and energetic properties of the small of nickel ions and molecules and provides reliable results for the nickel complexes. Calculations were performed using the Gaussian 09 Rev.D program [27]. Visualization of the computational results was performed in the VMD program [28]. To generate the wave functions of molecules and ions under study, we used the restricted Kohn–Sham method (wave functions for the closed electron shells). All calculations were performed for the standard conditions (298.15 K, 1 atm). As the initial structures, we used spherical face-centered cubic (*fcc*) clusters obtained by cutting the sphere of the ideal *fcc* lattice. Different spin states (singlet, triplet, quintet, septet,n, undetsimet) have been tested to solve the problem of the ground state of Ni_6 cluster for each spin state.

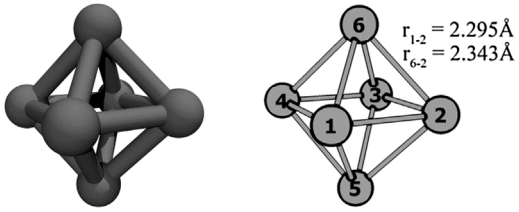

Fig. 1. The structure of 6-atom nickel nanocluster, the PBEH1PBE/Lanl2DZ calculations.

Table 1
Relative energies of the nanocluster Ni_6 in diverse spin states, the PBEH1PBE/Lanl2DZ calculations.

Multiplicity	Relative energy (kJ/mol)
1	510.44
3	118.35
5	54.35
7	7.74
9	0.00
11	107.32

Quantum-chemical modeling of the interaction of 4-propylheptane $C_{10}H_{22}$ with nanocluster Ni_6 was performed by the DFT method uωPBE0/Lanl2DZ_ecp in the TeraChem V. 1.9 program [29]. The results of this quantum-chemical simulation were used for analysis of weak interactions (RDG analysis) with the DFT method PBEH1PBE/Lanl2DZ implemented in the Multiwfn software package [30]. The critical points of the electron density (AIM analysis) was searched by the AIMAll 15.05.18 software package [31].

A molecular dynamics simulation of interaction between the Ni_6 nanocluster and 4-propylheptane $C_{10}H_{22}$ was performed based of the results obtained by the above-mentioned techniques. A computer experiment was implemented by *ab initio* Born-Oppenheimer molecular dynamics (BOMD) using the uωPBE/Lanl2DZ_ecp method in the TeraChem V. 1.9 program at 1500 °C. The high temperature is due to the specifics of the BOMD simulations and needed to accelerate the reaction of 4-propylheptane with Ni_6. To generate the wave functions of molecules, we used the unrestricted Kohn–Sham method (wave functions for the open electron shells). Electron shells of the transition metal were described by effective core pseudopotentials. The MD simulation of the Ni_6–$C_{10}H_{22}$ system was performed within the NVT ensemble using a 1 fs step and 20 ps as a total time of the simulation. The velocity scaling thermostat was applied to maintaining the constant temperature of the system.

All the calculations were performed on the cluster supercomputer of Institute of Petroleum Refining and Petrochemistry.

3. Results and discussion

The results of geometry optimization of the Ni_6 nanocluster are shown in Fig. 1 and Table 1. This entity is a trigonal bipyramid with a group D_{4h} symmetry.

To define the multiplicity of the ground state of Ni6, we have scrutinized Ni6 in diverse spin states and found that the nanocluster

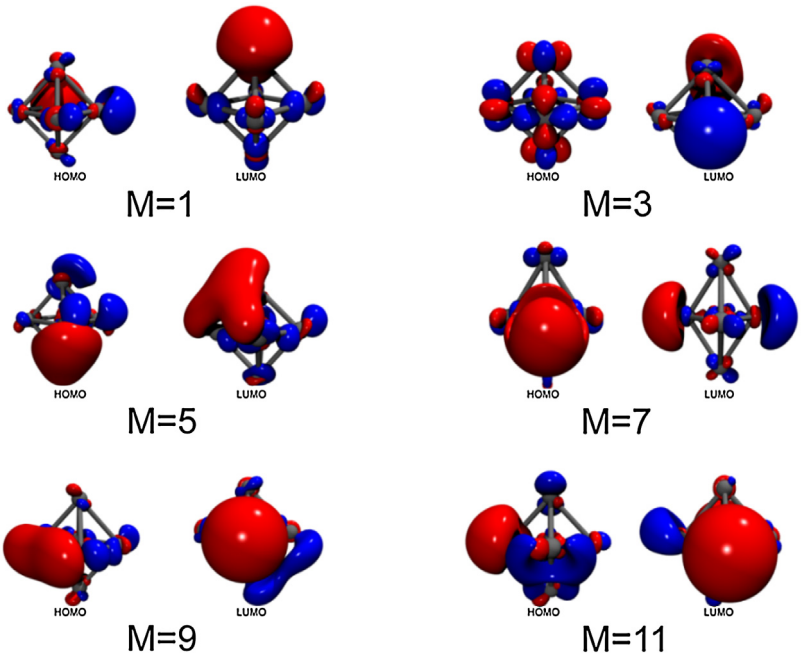

Fig. 2. HOMOs and LUMOs of the Ni_6 nanocluster.

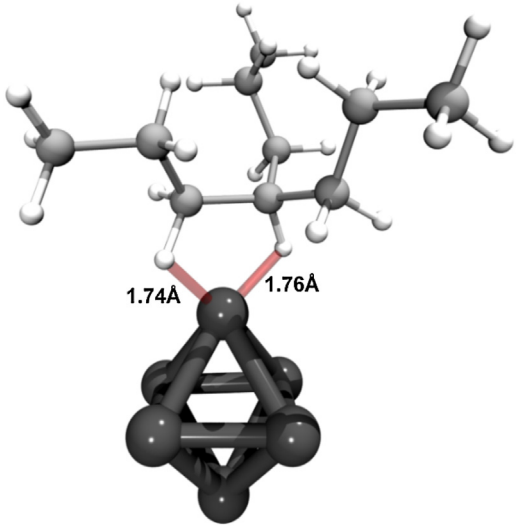

Fig. 3. Structure of the $Ni_6C_{10}H_{22}$ pre-reactionary complex.

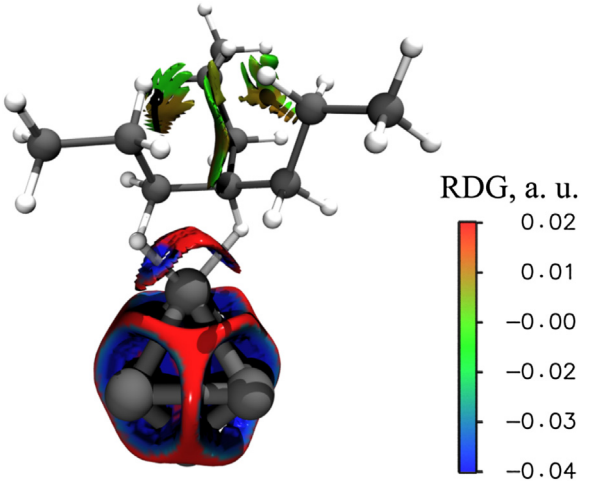

Fig. 4. Isosurfaces corresponding to the non-covalent interactions in the $Ni_6C_{10}H_{22}$ pre-reactionary complex.

with multiplicity 9 has the lowest total energy, i.e. it is the ground state.

Based on this data, the plot of the total energy of nanocluster versus its multiplicity has been obtained. Thus, the energy minimum corresponds to M = 9.

Key structural and energetic parameters of the Ni_6 nanocluster in diverse spin states are collected in Table 2. As found, the Ni_6 with M = 9 has the largest HOMO-LUMO gap, so it obey the HOMO-LUMO criterion of stability. The obtained computational value of corresponds to the crystal band gap measured in experimental work.

Fig. 2 represents the HOMOs and LUMOs for each of the spin states of Ni_6. The shape if the orbitals differ depending on multiplicity.

A complex between 4-propylheptane and Ni_6 is shown in Fig. 3. Red color indicates the hydrogen bonds between nickel and hydrogen atoms.

To confirm the hypotheses about the hydrogen bonds between nickel and hydrogen atoms of $C_{10}H_{22}$, we have performed the RDG-analysis of weak interactions and the AIM-analysis of critical points.

A new approach to the description of non-covalent interactions, based on a reduced density gradient the electron density (RDG) has been previously worked out This approach exploits the electron density and its derivatives to simultaneously visualize and analyze a wide range of non-covalent interactions as the real surfaces in space. The RDG calculations allows visualizing areas of non-covalent interactions in the formed complex $Ni_6C_{10}H_{22}$ (Fig. 4), which were colored according to the values of the sign of the second eigenvalue of the Hessian and the electron density (sign $(\lambda_2)\rho$). These values are used as estimates of the interaction strength. The sign of the second eigenvalue of the Hessian (sign $(\lambda_2)\rho$) indicates whether the interaction is bonding or nonbonding and electron density (ρ) assesses its strength. The gradient isosurfaces of weak interactions in the Ni6C10H22 complex are colored according to blue-green-red scale in the range of sign $(\lambda_2)\rho = -0.04...0.02$ a.u.

Table 2
Key structural and energetic parameters of the Ni_6 nanocluster in diverse spin states.

Parameter	Multiplicity					
	1	3	5	7	9	11
Bond length Ni_1-Ni_6 (Å)	2337	2438	2501	2989	2546	2396
HOMO level (eV)	−4,19	−5,68	−4,95	−4,78	−4,85	−4,35
LUMO level (eV)	−2,32	−2,95	−3,33	−3,25	−1,51	−2,96
HOMO-LUMO gap (eV)	1,86	2,73	1,62	1,53	3,34	1,39

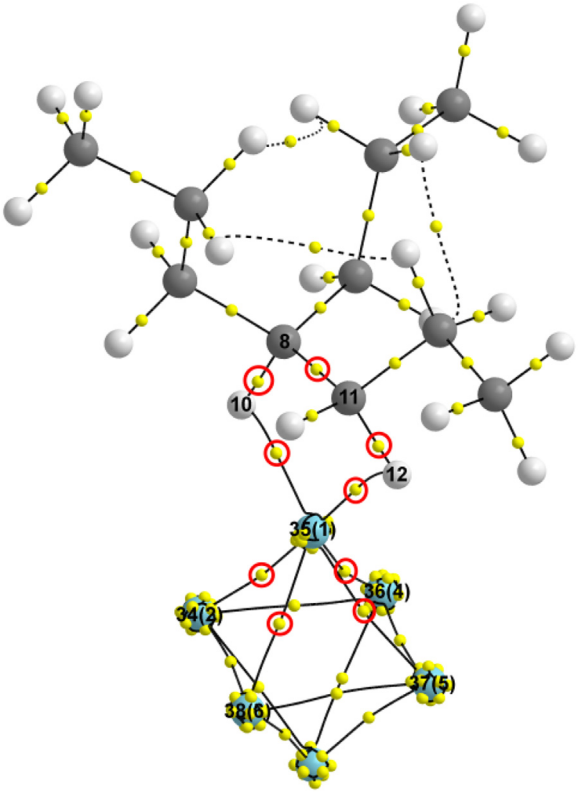

Fig. 5. Distribution of the Laplacian of the electron density of chemical bonds in the $Ni_6C_{10}H_{22}$ complex.

(Fig. 4). The isosurfaces corresponding to weak interactions are shown in blue. These interactions have attractive nature, which includes dipole–dipole interactions and hydrogen bonding, and characterized with high negative values. Such areas have a value greater than −0.04 a.u. and observed between the nickel atoms in the nanocluster and on the line of interaction between the hydrogen atoms in the $C_{10}H_{22}$ moiety of the formed pre-reactionary complex. Thus, we can conclude that the interactions Ni···H are not weak. Isosurfaces of interaction in the molecule of 4-propylheptane having sign $(\lambda_2)\rho = -0.005...-0.010$ a.u. are marked in green and correspond to weak Van der Waals forces. If the interaction is characterized with a large and positive sign $(\lambda_2)\rho$, it is considered repulsive (and colored in red). Such interactions can be found in the Ni_6 nanocluster in the centers of triangles and pentagon, which atoms participate in a donor-acceptor interaction between two hydrogen atoms and Ni atom. This is associated with the constraints of these cycles. Thus, the performed RDG analysis allows visualizing the interactions and indicating their type and strength.

An important parameter of chemical bond is the value of the Laplacian of the electron density at the bond critical point of contact: it is defined by the ratio between negative and positive eigenvalues of the Hessian λ1, λ2 and λ3, and thus depends on the nature of the chemical bond. This parameter allows classifying all atomic interactions into two groups depending on the distribution of the electron density between the nuclei. If the electron density is characterized by the dominance of negative curvature ($\nabla^2\rho_0$), the electron density is shifted to each of the interacting atoms and concentrated in the atomic basins. This reflects the effect of the Pauli principle. Such interactions are considered to be atomic interactions of the type of closed shells. To make a similar determination of ionic, hydrogen and van der Waals bonds, separating them from each other, it is currently not possible. All of these bonds are characterized by positive values of the electron density at the bond critical point, so they are considered jointly within a topological analysis (and called the closed shells like interactions).

The general picture of the Laplacian of the electron density distribution in the diverse chemical bonds is shown in Fig. 5. The bond critical points between nickel and hydrogen atoms are of the type (3, −1), which refers to the necessary condition for the formation of a strong bond between the atoms. Thus, the proposition about the strong bonding between the nickel nanocluster and 4-propylheptane is confirmed within two different theories.

According to the calculated Bader atomic charges for 4-propylheptane (Table 1 in Supplementary Material), the charge transfer 0.45 eV occurs when the complex between the Ni_6 nanocluster and $C_{10}H_{22}$ is formed. Information about the bond critical points in the nanocluster Ni6, hydrocarbon C10H22, and their complex is presented in Table 3. For convenience, we present only the key bond critical points in Fig. 5. Since the charge transfer occurs from the hydrocarbon molecule to the nickel nanocluster, the values of electron density in the bond critical points of $C_{10}H_{22}$ are reduced whereas the electron density values of bond critical points of the nanocluster is increased (Table 3).

Molecular modeling possesses a detailed picture of the processes in the system. During diverse calculations, characteristics of the molecular system are recorded, such as pair radial distribution function and preferential orientation of molecules in space. Fig. 6 describes the mobility of all hydrogen atoms in the molecule of 4-propylheptane when it interacts with Ni_6. Four lower peaks of the plot correspond to the separation of the elimination of the H atoms that have occurred upon the simulation (Fig. 6a). Fig. 6b shows the dependence of free energy on the length of the hydrogen atoms detached upon the simulation.

Key snapshots of four reactions are displayed in Fig. 7. The quantum-dynamical modeling reveal the following transformations the system undergo. At 11770 fs abstraction of the H atom of $C_{10}H_{22}$ and Ni of the nanocluster occur. These lead to the particles NiH, Ni_5, and $C_{10}H_{21}$ radical. The further hydrogen abstraction from the C10H21 radical at 12770 fs results in two NiH particles, Ni4, and biradical $C_{10}H_{20}$. At 14650 fs, the hydrogen atoms is abstracted from $C_{10}H_{20}$ leading to three NiH, Ni_3, and $C_{10}H_{19}$. Finally (19670 fs), the $C_{10}H_{19}$ particle losses the fourth H atom forming four NiH, Ni_2 and $C_{10}H_{18}$. Such processes are attributed to the first steps of cracking.

4. Conclusion

Recently, intensive research works on small particles (clusters) with dimensions ranging from dozens to thousands of

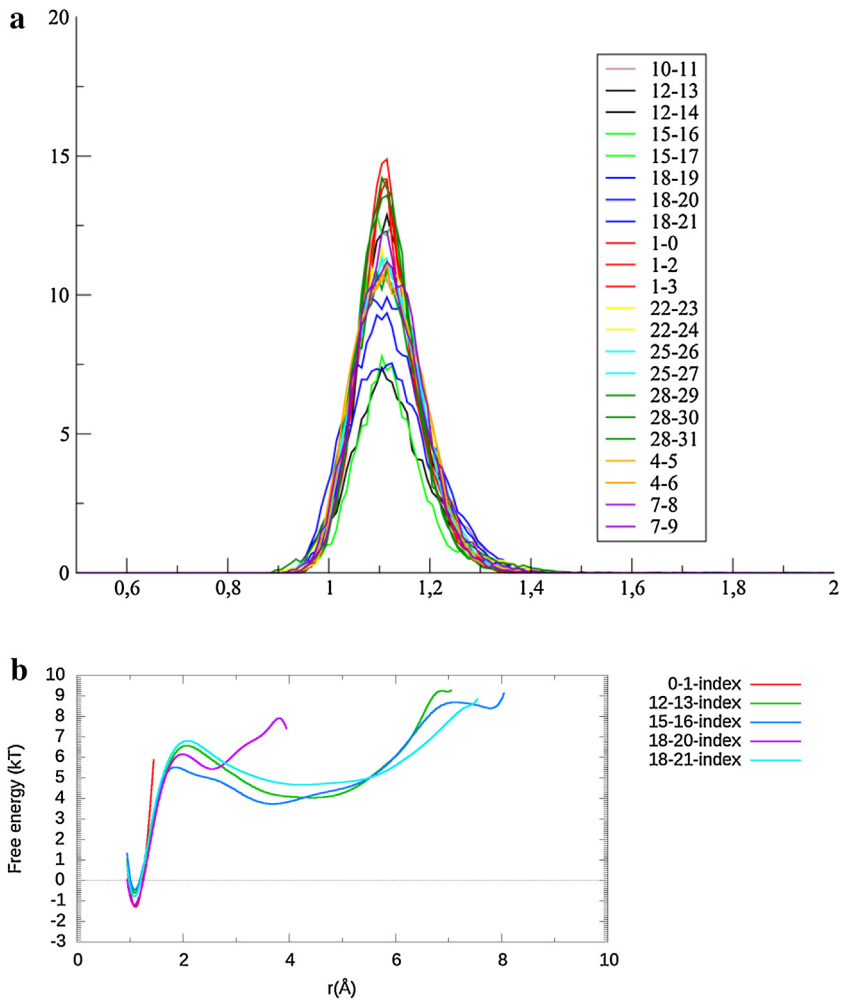

Fig. 6. a) Pair radial distribution function g(r) carbon (C) – hydrogen (H) at 1500 °C, the uωPBE0/Lanl2DZ_ecp method. b) Pair radial distribution function g(r) carbon (C) – hydrogen (H) at 1500 °C as a dependence of free energy on the bond length, the uωPBE0/Lanl2DZ_ecp calculations.

Table 3
Characteristics of atomic interactions in the bond critical points of the compounds under study (all values are given in atomic units).

Compound	BCP	Atoms	ρ_0	$\nabla^2\rho_0$	Ellipticity
Ni_6	1	Ni1 – Ni2	+0.038405	+0.067302	+0.365700
	3	Ni1 – Ni4	+0.038405	+0.067303	+0.365698
	5	Ni1 – Ni5	+0.044269	+0.125646	+0.069508
	9	Ni1 – Ni6	+0.044269	+0.125646	+0.069508
$C_{10}H_{22}$	9	C8 – H10	+0.268546	−0.935301	+0.006191
	10	C8 – C11	+0.238569	−0.535010	+0.006546
	11	C11 – H12	+0.272178	−0.952975	+0.000084
$Ni_6C_{10}H_{22}$	1	C8 – H10	+0.222504	−0.529601	+0.019114
	11	C8 – C11	+0.212661	−0.384369	+0.010084
	14	C11 – H12	+0.221623	−0.521026	+0.016560
	37	Ni35 – Ni38	+0.052354	+0.119612	+0.399127
	38	Ni34 – Ni35	+0.046658	+0.115210	+0.418890
	40	Ni35 – Ni37	+0.052609	+0.151805	+0.194081
	42	Ni35 – Ni36	+0.048949	+0.125710	+0.247061

atoms are performed. However, the experimental study of nanoclusters encounters certain difficulties related mainly to the small particle size. Therefore, one of the possible approaches to studying nanoscale objects is based on computer simulation models. Theoretical modeling with the PBEH1PBE/Lanl2DZ method allowed obtaining structural parameters of the Ni_6 nanocluster, and determining multiplicity of its ground state and accompanying molecular characteristics. The most promising for the study of the properties of metal clusters, in our opinion, is the method of molecular dynamics, which allows defining the influence of various factors on the properties of these particles at the atomic level. Accordingly, the molecular dynamics simulation of nanocluster Ni_6 with 40propylheptane was performed as a theoretical model of initial processes of the catalytic cracking of vacuum gas oil. According to the results of the simulation, chemical bonds between the nickel atom of Ni_6 and hydrogen atoms of C10H22 are formed. To support of this hypothesis, the RDG analysis of weak interactions and AIM-analysis of the electron density of the bond critical points were performed. Both analyses confirmed the formation of the Ni-H bond.

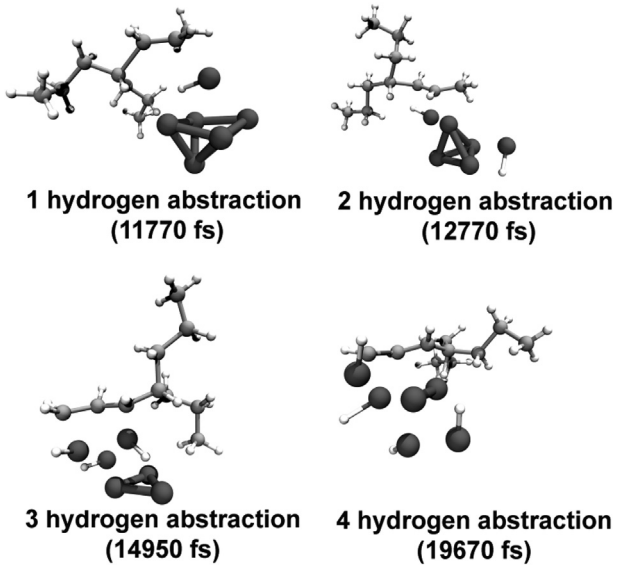

Fig. 7. Interaction of the Ni_6 nanocluster with the branched molecule $C_{10}H_{22}$. Snapshots correspond to the subsequent hydrogen abstractions.

Acknowledgment

This study was conducted with support from the Russian Science Foundation within project No. 15-13-00115.

Appendix A. Supplementary data

Supplementary data associated with this article can be found, in the online version, at http://dx.doi.org/10.1016/j.jmgm.2016.12.017.

References

[1] R. Pou-Amérigo, M. Merchán, I. Nebot-Gil, P.Å. Malmqvist, B.O. Roos, The chemical bonds in CuH, Cu2, NiH, and Ni2 studied with multiconfigurational second order perturbation theory, J. Chem. Phys. 101 (1994) 4893–4902.
[2] P. St Petkov, G.N. Vayssilov, S. Kruger, N. Rosch, Structure, stability, electronic and magnetic properties of Ni4 clusters containing impurity atoms, Phys. Chem. Chem. Phys. 8 (2006) 1282–1291.
[3] M.B. Knickelbein, S. Yang, S.J. Riley, Near-threshold photoionization of nickel clusters: ionization potentials for Ni3 to Ni90, J. Chem. Phys. 93 (1990) 94–104.
[4] L. Chenglin, The structure of small nickel clusters: ni2 −Ni19, Modell. Simul. Mater. Sci. Eng. 8 (2000) 95.
[5] J.A.M. Simoes, J.L. Beauchamp, Transition metal-hydrogen and metal-carbon bond strengths: the keys to catalysis, Chem. Rev. 90 (1990) 629–688.
[6] A. Kant, Dissociation energies of diatomic molecules of the transition elements. I. Nickel, J. Chem. Phys. 41 (1964) 1872–1876.
[7] O. Ovsitser, E.V. Kondratenko, Similarity and differences in the oxidative dehydrogenation of C2–C4 alkanes over nano-sized VOx species using N2O and O2, Catal. Today 142 (2009) 138–142.
[8] J.C. Pinegar, J.D. Langenberg, C.A. Arrington, E.M. Spain, M.D. Morse, Ni_2 revisited: reassignment of the ground electronic state, J. Chem. Phys. 102 (1995) 666–674.
[9] F.A. Reuse, S.N. Khanna, Geometry, electronic structure, and magnetism of small Ni_n (n = 2–6, 8, 13 clusters, Chem. Phys. Lett. 234 (1995) 77–81.
[10] F.A. Reuse, S.N. Khanna, Photoabsorption spectrum of small nin (n = 2-6, 13) clusters, Eur. Phys. J. D 6 (1999) 77–81.
[11] J. Uddin, C.M. Morales, J.H. Maynard, C.R. Landis, Computational studies of metal-ligand bond enthalpies across the transition metal series, Organometallics 25 (2006) 5566–5581.
[12] E.K. Parks, L. Zhu, J. Ho, S.J. Riley, The structure of small nickel clusters. I. Ni3–Ni15, J. Chem. Phys. 100 (1994) 7206–7222.
[13] M. Moskovits, J.E. Hulse, The ultraviolet–visible spectra of diatomic, triatomic, and higher nickel clusters, J. Chem. Phys. 66 (1977) 3988–3994.
[14] M.A. Nygren, P.E.M. Siegbahn, U. Wahlgren, H. Aakeby, Theoretical ionization energies and geometries for nickel (Nin 4.ltoreq. n.ltoreq. 9), J. Phys. Chem. 96 (1992) 3633–3640.
[15] K.P. Jensen, B.O. Roos, U. Ryde, Performance of density functionals for first row transition metal systems, J. Chem. Phys. 126 (2007) 014103.
[16] F. Furche, J.P. Perdew, The performance of semilocal and hybrid density functionals in 3d transition-metal chemistry, J. Chem. Phys. 124 (2006) 044103.
[17] J.G. Harrison, Density functional calculations for atoms in the first transition series, J. Chem. Phys. 79 (1983) 2265–2269.
[18] G. López Arvizu, P. Calaminici, Assessment of density functional theory optimized basis sets for gradient corrected functionals to transition metal systems: the case of small nin($n \leq 5$) clusters, J. Chem. Phys. 126 (2007) 194102.
[19] M.C. Michelini, R. Pis Diez, A.H. Jubert, Density functional study of the ionization potentials and electron affinities of small Nin clusters with n = 2–6 and 8, Comput. Mater. Sci 31 (2004) 292–298.
[20] I. Onal, A. Sayar, A. Uzun, S. Ozkar, A density functional study of ni2 and ni13 nanoclusters, J. Comput. Theor. Nanosci. 6 (2009) 867–872.
[21] J.P. Perdew, K. Burke, M. Ernzerhof, Generalized gradient approximation made simple, Phys. Rev. Lett. 77 (1996) 3865–3868.
[22] J.P. Perdew, K. Burke, M. Ernzerhof, Generalized gradient approximation made simple [Phys. rev. lett. 77, 3865 (1996)], Phys. Rev. Lett. 78 (1997) 1396.
[23] T.H. Dunning, P.J. Hay, Gaussian basis sets for molecular calculations, in: H.F. Schaefer (Ed.), Methods of Electronic Structure Theory, Springer, US, Boston, MA, 1977, pp. 1–27.
[24] P.J. Hay, W.R. Wadt, Ab initio effective core potentials for molecular calculations. Potentials for the transition metal atoms Sc to Hg, J. Chem. Phys. 82 (1985) 270–283.
[25] W.R. Wadt, P.J. Hay, Ab initio effective core potentials for molecular calculations. Potentials for main group elements Na to Bi, J. Chem. Phys. 82 (1985) 284–298.
[26] P.J. Hay, W.R. Wadt, Ab initio effective core potentials for molecular calculations. Potentials for K to Au including the outermost core orbitals, J. Chem. Phys. 82 (1985) 299–310.
[27] M.J. Frisch, G.W. Trucks, H.B. Schlegel, G.E. Scuseria, M.A. Robb, J.R. Cheeseman, G. Scalmani, V. Barone, B. Mennucci, G.A. Petersson, H. Nakatsuji, M. Caricato, X. Li, H.P. Hratchian, A.F. Izmaylov, J. Bloino, G. Zheng, J.L. Sonnenberg, M. Hada, M. Ehara, K. Toyota, R. Fukuda, J. Hasegawa, M. Ishida, T. Nakajima, Y. Honda, O. Kitao, H. Nakai, T. Vreven, J. Montgomery, J.A, J.E. Peralta, F. Ogliaro, M. Bearpark, J.J. Heyd, E. Brothers, K.N. Kudin, V.N. Staroverov, R. Kobayashi, J. Normand, K. Raghavachari, A. Rendell, J.C. Burant, S.S. Iyengar, J. Tomasi, M. Cossi, N. Rega, J.M. Millam, M. Klene, J.E. Knox, J.B. Cross, V. Bakken, C. Adamo, J. Jaramillo, R. Gomperts, R.E. Stratmann, O. Yazyev, A.J. Austin, R. Cammi, C. Pomelli, J.W. Ochterski, R.L. Martin, K. Morokuma, V.G. Zakrzewski, G.A. Voth, P. Salvador, J.J. Dannenberg, S. Dapprich, A.D. Daniels, Ö. Farkas, J.B. Foresman, J.V. Ortiz, J. Cioslowski, D.J. Fox, Gaussian 09, Revision D.1, Gaussian Inc, Wallingford, CT, 2009.
[28] W. Humphrey, A. Dalke, K. Schulten, VMD: visual molecular dynamics, J. Mol. Graphics 14 (1996) 33–38.
[29] I.S. Ufimtsev, T.J. Martinez, Quantum chemistry on graphical processing units. 3. Analytical energy gradients, geometry optimization, and first principles molecular dynamics, J. Chem. Theor. Comp. 5 (2009) 2619–2628.
[30] T. Lu, F. Chen, Multiwfn A multifunctional wavefunction analyzer, J. Comp. Chem. 33 (2012) 580–592.
[31] T.A. Keith, AIMAll, 2008.